Effect of a strongly magnetized plasma on the resonant photon scattering process

Effect of a strongly magnetized plasma on the resonant photon scattering process

M V Chistyakov[1], **D A Rumuyantsev**[1] **and A A Yarkov**[1,2]

[1] Division of Theoretical Physics, Department of Physics, P.G. Demidov Yaroslavl State University, Sovietskaya 14, 150000 Yaroslavl, Russian Federation

[2] Yaroslavl Higher Military School of Air Defense, Yaroslavl Branch, Moskovskiy Prosp. 28, 150001 Yaroslavl, Russian Federation

E-mail: `a121@mail.ru`

Abstract. In this paper, the photons absorption rate in a relatively strong magnetic field in the Compton process taking into account the resonance on the virtual electron are calculated. A comparative analysis of the obtained result with the nonresonant case was carried out.

1. Introduction

It is the established fact that the presence of a magnetic field in a wide class of astrophysical objects is a typical situation for the observable universe. The scale of the magnetic induction can vary over a very wide range: from large-scale ($\sim$ 100 kpc) intergalactic magnetic field $\sim 10^{-21}$ G. [1], to the fields that are realized in the scenario of a rotational supernova explosion $\sim 10^{17}$ G. In this case, objects with a fields scale of the so-called critical value are of particular interest: $B_e = m^2/e \simeq 4.41 \times 10^{13}$ G. [1] These include, in particular, isolated neutron stars, which include radio pulsars and the so-called magnetars, which have magnetic fields with induction from $B \sim 10^{12}$ G (radio pulsars) to $B \sim 10^{15}$ G (magnetars).

An analysis of the emission spectra of radio pulsars and magnetars also indicates the presence of an electron-positron plasma in their magnetospheres with a concentration of the order of the Goldreich-Julian concentration [2]:

$$n_{GJ} \approx 3 \cdot 10^{13} \mathrm{cm}^{-3} \frac{B}{100 B_e} \frac{10s}{P}\,, \tag{1}$$

where P is the rotation period of the neutron star.

It is natural to expect that such extreme conditions will have a significant impact on quantum processes, where in the final or initial condition can be present both electrically charged and electrically neutral particles such as electrons and photons. One of the brightest representatives of reactions of this type is the process of Compton scattering of photons by electrons (positrons) magnetized medium, $\gamma e \to \gamma e$. This research dates back to the 30s of the twentieth century and has not stopped yet (see, for example, [3,4]). It should be noted that in all of these studies, the calculations were performed without taking into account the effect on the dispersion properties of photons. In relatively recent papers [5,6], the limit of a strongly magnetized charge symmetric

[1] We use the natural units $c = \hbar = k = 1$, m is the electron mass, $e > 0$ is the elementary charge.

and degenerate plasma was investigated. It was shown that taking into account the dispersion and renormalization of the photon wave functions leads to a significant modification of the photon absorption coefficients. However, in [5, 6], the situation when the scattering reaction will proceed taking into account the resonance on the virtual electron was not considered. Also, recently, the resonance effect in the Compton process as applied to the physics of radio pulsars was actively discussed in the literature [7–11].

Under such conditions, it is of interest to consider the Compton scattering reaction taking into account the possible resonance on a virtual electron, taking into account the change in the polarization and dispersion properties of the photon.

2. Photon absorption rate in the strong magnetic field

In a magnetized plasma, in the general case, a photon will have elliptical polarization and 3 polarization states.

In the limit $B \gtrsim B_e$ and in case of charge symmetric plasma ($\mu = 0$), polarization vectors will have the same form as in a pure magnetic field:

$$\varepsilon^{(1)}_\mu = \frac{(\varphi q)_\mu}{\sqrt{q^2_\perp}}, \;\; \varepsilon^{(2)}_\mu = \frac{(\tilde{\varphi} q)_\mu}{\sqrt{q^2_{\shortparallel}}}, \tag{2}$$

where q^μ and q'^μ are the momenta of the initial and final photons [2].

The following designations were used in this work: $(ab)_\perp = a_x b_x + a_y b_y$, $(ab)_{\shortparallel} = a_0 b_0 - a_z b_z$, $(a\varphi b) = a_y b_x - a_x b_y$. $\varphi_{\alpha\beta} = F_{\alpha\beta}/B$ and $\tilde{\varphi}_{\alpha\beta} = \frac{1}{2}\varepsilon_{\alpha\beta\mu\nu}\varphi_{\mu\nu}$ is the dimensionless field tensor and dual tensor, respectively.

Kinematic analysis taking into account the dispersion properties of the photon shows that 4 partial photon scattering channels are possible $e\gamma^{(1)} \to e\gamma^{(1)}$, $e\gamma^{(2)} \to e\gamma^{(2)}$, $e\gamma^{(2)} \to e\gamma^{(1)}$ and $e\gamma^{(1)} \to e\gamma^{(2)}$.

In addition, it follows from the dispersion properties of a photon in a magnetic field that a photon of mode 2 in the region $q^2_{\shortparallel} \geqslant 4m^2$ is unstable and can decay into a pair [12]. On the other hand, the mode 1 photon is stable in the region $0 \leq q^2_{\shortparallel} \leq (\sqrt{m^2 + 2eB} + m)^2$, which certainly falls into the resonance region $q^2_{\shortparallel} \gtrsim (\sqrt{m^2 + 2eB} - m)^2$ Therefore, to study the resonance taking into account the photon stability, it is sufficient to consider the channels $e\gamma^{(1)} \to e\gamma^{(1)}$ and $e\gamma^{(1)} \to e\gamma^{(2)}$

The amplitude which takes into account the finite width of electron absorption can be obtained from the results of [5] and presented in the following form:

$$\begin{aligned} \mathcal{M}_{\lambda \to \lambda'} &= -4\pi\alpha \exp\left[-\frac{q^2_\perp + q'^2_\perp - 2i(q\varphi q')}{4eB}\right] \times \\ &\times \sum_{n=0}^{\infty} \frac{\varepsilon^{*(\lambda')}_\alpha(q')\varepsilon^{(\lambda)}_\beta(q) T^n_{\alpha\beta}}{q^2_{\shortparallel} + 2(pq)_{\shortparallel} - 2eBn + i(E+\omega)\Gamma_n} + \\ &+ (q \leftrightarrow -q') \end{aligned} \tag{3}$$

Here Γ_n is the total electron absorption width [12], $T^n_{\alpha\beta}$ is the regular value (see [5]), p^μ and p'^μ are the momenta of the initial and final electron.

Let us determine the photon absorption coefficient according to work [5]:

$$\begin{aligned} W_{\lambda e \to \lambda' e} &= \frac{eB}{16(2\pi)^4 \omega_\lambda} \int |\mathcal{M}_{\lambda\to\lambda'}|^2 Z_\lambda Z_{\lambda'} \times \\ &\times f_E(1 - f_{E'})(1 + f_{\omega'})\delta(\omega_\lambda(\mathbf{k}) + E - \omega_{\lambda'}(\mathbf{k}'))\frac{dp_z d^3k'}{EE'\omega_{\lambda'}}. \end{aligned} \tag{4}$$

[2] Symbols 1 and 2 correspond to X - and O - modes at work [7],

and carry out a numerical analysis of the absorption coefficient in comparison with the δ-functional approximation taken from [8].

In equation (4), $\lambda, \lambda' = 1, 2$, $f_\omega = [\exp(\omega/T) - 1]^{-1}$, $f_E = [\exp(E/T) + 1]^{-1}$ are the equilibrium distribution functions of photons and electrons, E and E' are the energies of the initial and final electrons, respectivel,

$$\varepsilon_\alpha^{(\lambda)}(q) \to \varepsilon_\alpha^{(\lambda)}(q)\sqrt{Z_\lambda}, \quad Z_\lambda^{-1} = 1 - \frac{\partial \mathcal{P}^{(\lambda)}(q)}{\partial \omega^2}, \tag{5}$$

$\mathcal{P}^{(\lambda)}(q)$ is the eigenvalue of polarization operator for the mode λ photon.

3. Numerical analysis

Comparative analysis of the probability of scattering in the case of resonance (solid line), work [5] (dotted line) and interpolation δ-function marked with dots.

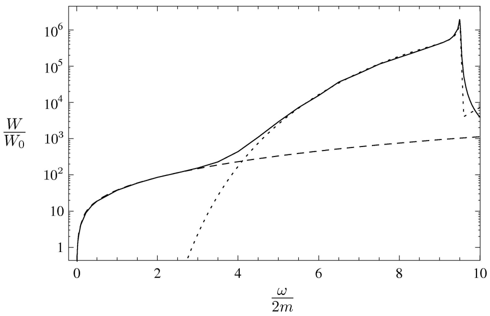

Figure 1. Photon absorption rate vs the frequency of the initial photon for the $1 \to 1$ channel at a field $B = 200B_e$ and a temperature T=1 MeV. The solid and dashed lines show the graph with and without resonance, respectively. δ-functional approximation is showed by a dotted line. Here $W_0 = (\alpha/\pi)^3 m \simeq 3.25 \cdot 10^2$ cm^{-1}.

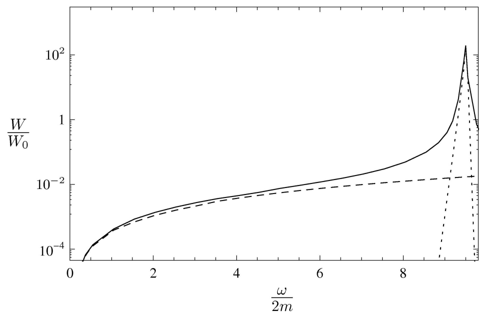

Figure 2. The same plot as in figure 1, but for the $1 \to 1$ channel at a field $B = 200B_e$ and a temperature T=50 keV.

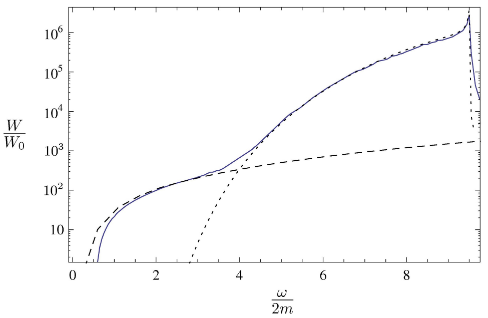

Figure 3. The same plot as in figure 1, but for the $1 \to 2$ channel at a field $B = 200B_e$ and a temperature T=1 MeV.

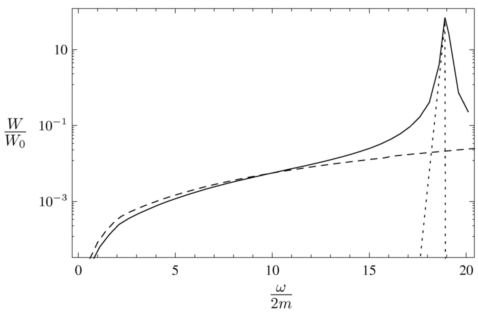

Figure 4. The same plot as in figure 1, but for the $1 \to 2$ channel at a field $B = 200B_e$ and a temperature T=50 keV.

Analysis of figures 1-2 shows that photon absorption rate for channel $\gamma^{(1)}e \to \gamma^{(1)}e$ agrees with appropriate result for the strong magnetic field limit and without resonance, obtained in the work [5] up to the energies of the initial photon $\omega = 3$ MeV for $B = 200B_e$ and $\omega = 0.3$ MeV for $B = 20B_e$. The overestimation of the absorption rate at low energies of the initial photon is most clearly seen from figures 3-4. It happens is due to the fact that in the strong magnetic field limit the non-resonant case was considered in the work [5]. In addition, it follows from the figures 3 and 1 that the δ-function approximation works well enough. Numerical analysis shows that the main contribution to the error comes from the peak area. The δ-function approximation provides a good approximation for absorption rate of photons in the area of resonances with precision up to 7% (figure 1), 49% (figure 2), 9% (figure 3) and 16% (figure 4). Note, that δ-function approximation at relatively low temperatures works worse.

4. Summary

The cross section is calculated and compared with the results available in the literature. It is shown that in case of high temperatures $T > m$, the resonance starts to contribute to the photon absorption coefficient earlier than assumed in the work [5]. In particular, for a magnetic field with $B = 200B_e$ and temperature $T = 1$ MeV, the results of work [5] should be limited to photon energies of $\omega \sim 4$ MeV.

It is shown that the δ-functional approximation of the resonance peaks at a temperature of $T \sim 1$ MeV in the resonance region is in a good agreement with the relevant results [7] obtained by the cumbersome numerical calculations. At a temperature of $T \sim 50$ keV, the δ-functional approximation works worse, since the peak becomes narrower and the resonance effect occurs later.

Acknowledgments

The work was funded by RFBR, project number 20-32-90068.

References

[1] Ryu D, Schleicher D R G, Treumann R A, Tsagas C G and Widrow L M 2012 *Space Sci. Rev.* **166** 1–35
[2] Goldreich P and Julian W H 1969 *Astrophys. J.* **157** 869–80
[3] Herold H 1979 *Phys. Rev.* D **19** 2868–75
[4] Melrose D B and Parle A J 1983 *Aust. J. Phys.* **36** 799–824
[5] Chistyakov M V and Rumyantsev D A 2009 *Int. J. Mod. Phys.* A **24** 3995–4008
[6] Chistyakov M V, Rumyantsev D A and Stus' N S 2012 *Phys. Rev.* D **86** 043007
[7] Mushtukov A A, Nagirner D I and Poutanen J 2016 *Phys. Rev.* D **93** 105003
[8] Rumyantsev D A, Shlenev D and Yarkov A 2017 *J. Exp. Theor. Phys.* **125** 410–9
[9] Wadiasingh Z, Baring M G, Gonthier P L and Harding A K 2018 *Astrophys. J.* **854** 98
[10] Kostenko A and Thompson C 2018 *Astrophys. J.* **869** 44
[11] Philippov A, Timokhin A and Spitkovsky A 2020 *Phys. Rev. Lett.* **124** 245101
[12] Kuznetsov A V and Mikheev N V 2003 *Electroweak processes in external electromagnetic fields* (New York: Springer-Verlag)